Surface Science 603 (2009) 60–64

Contents lists available at ScienceDirect

Surface Science

journal homepage: www.elsevier.com/locate/susc

Water adsorption on hydrogenated Si(1 1 1) surfaces

B. Lange [a], R. Posner [a], K. Pohl [a], C. Thierfelder [b], G. Grundmeier [c], S. Blankenburg [d], W.G. Schmidt [d,*]

[a] *Max-Planck-Institut für Eisenforschung GmbH, Max-Planck-Straße 1, 40237 Düsseldorf, Germany*
[b] *Centre of Theoretical Chemistry and Physics, Massey University, Private Bag 102904, North Shore MSC, Auckland, New Zealand*
[c] *Lehrstuhl für Technische und Makromolekulare Chemie, Universität Paderborn, 33095 Paderborn, Germany*
[d] *Lehrstuhl für Theoretische Physik, Universität Paderborn, 33095 Paderborn, Germany*

ARTICLE INFO

Article history:
Received 1 October 2008
Accepted for publication 14 October 2008
Available online 5 November 2008

Keywords:
Density functional calculations
Contact angle measurements
Water adsorption
Wetting
Si(1 1 1):H

ABSTRACT

The adsorption of water on the hydrogen terminated Si(1 1 1) surface is studied by means of *first-principles* calculations as well as contact angle measurements. Possible initial adsorption configurations for single water molecules and the potential energy surface are calculated. Only small adsorption energies of the order of meV are predicted. Calculations for higher coverage show that the water–water interactions are stronger than the water–surface bonding. The contact angle formed between a water droplet on the surface approximated from the total-energy calculations amounts to 88°, while our measured value is 91°.

Despite substantial research efforts, the structural properties of water are incompletely understood. This holds for the ubiquitous liquid phase [1,2] as well as for thin substrate-supported water films and clusters prepared in the laboratory [3–6]. Even the hydrophilic/hydrophobic character of some simple, well-understood surfaces is not clear [7–9]. The interaction of water with solid surfaces, however, is of key importance for many chemical and physical processes [10–16]. In order to better understand the water–surface interaction, well defined model systems accessible to both surface-sensitive probes as well as *first-principles* calculations need to be investigated. The adsorption of water on the Si(1 1 1):H surface [8] presents such a case. We present *first-principles* calculations on the adsorption of single water molecules, water clusters and water thin films on the Si(1 1 1):H surface. The contact angle approximated from the total-energy calculations is compared with the value measured for a hydrogen terminated Si(1 1 1) wafer.

The calculations are performed using density functional theory (DFT) within the generalized gradient approach (GGA) as implemented in the Vienna *Ab initio* Simulation Package (VASP) [17]. The electron-ion interaction is described by the projector-augmented wave scheme [18]. The electronic wave functions are expanded into plane waves up to a kinetic energy of 400 eV. The surface is modeled by periodically repeated slabs. They contain nine Si bulk layers orientated along the [1 1 1] direction and a vacuum region of about 23 Å. We consider a (2 × 2) surface unit cell throughout this work. All calculations are performed using the calculated Si equilibrium lattice constant of 5.456 Å. The surface silicon dangling bonds are passivated with hydrogen. For the ionic relaxation we use the conjugate gradient method with a force truncation criterium of about 40 meV/Å. The Brillouin zone integration is performed using a 4 × 4 × 1 Monkhorst–Pack mesh.

We use the PW91 functional [20] to describe the electron exchange and correlation energy within the GGA. It describes the hydrogen bonds in solid water (ice Ih) in good agreement with experiment [21,22]. However, in the case of molecules weakly bonded to each other or to the surface, dispersion interaction – not accounted for in the GGA – may contribute a sizable percentage of the total interaction energy [23]. In order to assess at least approximately the influence of the van der Waals (vdW) interaction on the adsorption energetics, we present some additional data that are obtained using a semiempirical approach based on the London dispersion formula to include the dispersion interaction [24]. Due to the limitations inherent to this approach it should be considered to provide error bars and energetic trends rather than accurate results.

The influence of the dispersion or van der Waals (vdW) interaction on gas-phase water molecules is illustrated in Table 1. Here we compare the structural data calculated for the gas-phase water molecule within DFT and DFT supplemented with dispersion interaction with experiment. Obviously, within both approaches the measured geometry is well described. As one expects, the van der Waals interaction leads to a slight decrease of the H—O—H bond angle. For the vibration frequencies we find the DFT values to be closer to the experiment than the DFT + vdW results. This is

---

[*] Corresponding author. Fax: +49 5251/603435.
E-mail address: w.g.schmidt@upb.de (W.G. Schmidt).

0039-6028/$ - see front matter © 2008 Elsevier B.V. All rights reserved.
doi:10.1016/j.susc.2008.10.030

Table 1
O—H bond length (Å) and H—O—H bond angle calculated and measured for the gas-phase water molecule. Also given are the vibrational frequencies of the antisymmetric, symmetric and bending mode in cm^{-1}.

	Experiment [19]	DFT	DFT + vdW
O—H	0.958	0.97	0.97
H—O—H	104.45	104.7	104.0
Antisymmetric stretching	3756	3831	3837
Symmetric stretching	3657	3720	3798
Bending	1595	1580	1662

related to the somewhat arbitrary choice of the cutoff function that quenches the dispersion interaction for short bonding distances [24].

In addition to the calculations, contact angle measurements were performed. Thereby both side polished Si(111) wafers, *n*-type, *p*-doped, with a resistivity of 4000–6900 Ω cm were first cleaned in 1:1 30% NH_3/30% H_2O_2 solution at 80 °C and then carefully rinsed with ultrapure water. Hydrogen termination was achieved in freshly prepared 40% NH_4F solution during 8 min at room temperature. The surfaces were subsequently rinsed with ultrapure water and dried in a nitrogen stream. To minimize surface contaminations and/or re-oxidation of the surface, the samples were stored in ethanol (99.8%) or ultra high vacuum. Water contact angles were measured by means of a dataphysics system OCA 20 in a chamber with nitrogen atmosphere of controlled humidity. The relative humidity of either 1.2 ± 1.0% or 96.8 ± 1.0% at 23.0 ± 0.3 °C could be adjusted by means of a gas mixing system. 4 μl droplets of ultra purified water (pH = 6.9) were deposited with a dosing rate of 0.2 μl/s and measured in advancing mode. The surface conditions were checked by X-ray photoelectron spectroscopy (XPS) applying a Quantum 2000, Physical Electronics, USA. Spectra were measured at 45° using a monochromated Al Kα source at 93.9 eV pass energy and 0.8 eV step size for survey spectra and 23.5 eV pass energy at 0.2 eV step size for detailed spectra. Atomic force microscope (AFM) experiments were performed with a Digital Instruments Dimension 3100. Morphology images were recorded in tapping mode with a line rate of 1 Hz.

We start by determining the potential energy surfaces (PES) for a single water monomer adsorbed on the Si(111):H surface. Since the most favorable adsorption configuration is not clear *a priori* and we cannot expect the (rather weak) bonding forces to rotate the molecule in the most favorable orientation, we consider three different starting geometries for each lateral monomer position. The water molecule is oriented either with its oxygen atom down, with one hydrogen down and one hydrogen up, or with its molecular plane parallel to the surface. The latter orientation is often assumed on metal surfaces [16]. The results are shown in Fig. 1. Irrespective of the molecular orientation, the PES is rather flat with a maximum corrugation of 57 meV. The most favorable adsorption configurations yield energies of 30, 70, and 82 meV for the oxygen down, planar, and one hydrogen down orientation, respectively.

Consequently, we use the latter configuration as starting point for further calculations where we study higher coverages. The most favorable dimer configuration found here is shown in Fig. 2. We find the adsorption energy with respect to gas-phase molecules to increase upon dimer formation, from 82 to 191 meV, see Table 2. However, this increase in energy is related to the monomer–monomer interaction rather than the molecule–surface interaction. This becomes clear from the calculation of the binding energy per molecule, which we define as

$$E_{\mathrm{bind}} = \left(E_{\mathrm{surf}} + E_{(\mathrm{H_2O})_n} - E_{(\mathrm{H_2O})_n,\mathrm{surf}}\right)/n, \tag{1}$$

where E_{surf} and $E_{(\mathrm{H_2O})_n,\mathrm{surf}}$ are the energies of the clean and water adsorbed Si(111):H surfaces, respectively, and $E_{(\mathrm{H_2O})_n}$ represents the energy of the adsorbed water configuration, e.g., the water dimer, calculated in the same surface unit as the total system, but with the Si atoms missing. In the adsorption energy per molecule

$$E_{\mathrm{ads}} = \left(E_{\mathrm{surf}} + n \cdot E_{\mathrm{H_2O}} - E_{(\mathrm{H_2O})_n,\mathrm{surf}}\right)/n, \tag{2}$$

in contrast, $n \cdot E_{\mathrm{H_2O}}$ corresponds to n single water monomers in gas-phase. For the gas-phase calculations of water monomers a cubic $20 \times 20 \times 20$ Å cell was used. Due to the structural relaxation, the monomer adsorption and binding energies calculated according to this definition will differ.

As can be seen in Table 2, the surface binding energy even decreases upon dimer formation, at least within DFT. Adding the empirical vdW correction to the total-energy and force calculations, the balance of water–water and water–surface interactions somewhat shifts in favor of the latter. Now we observe a decrease of the adsorption energy and an increase of the binding energy upon dimer formation. The stronger interaction between water and the Si(111):H surface upon inclusion of dispersion forces does not only lead to adsorption energies that are significantly (by about 0.5 eV) higher than in DFT, but also manifests itself in stronger molecular distortions. While, for example, the H—O—H bond angle changes by less than 0.1° for adsorbed monomers and dimers within DFT, the corresponding changes in DFT + vdW are about 2°. Even more significant are the adsorption geometry changes upon inclusion of dispersion interaction. As an example, we show in Fig. 2 the minimum adsorption geometry for water monomers both in DFT and DFT + vdW. The latter is more planar. Also the surface–molecule distance is affected. Within DFT/DFT + vdW we obtain minimum distances of 2.04/1.61 and 2.47/1.57 Å for the monomer and the dimer, respectively.

The adsorption of water also modifies its vibrational frequencies. We calculate (within DFT) shifts of −38, −46, and 24 cm^{-1} for the antisymmetric and symmetric stretching and bending mode of the monomer, respectively. According to the calculations, the most obvious vibrational fingerprint for the formation of water

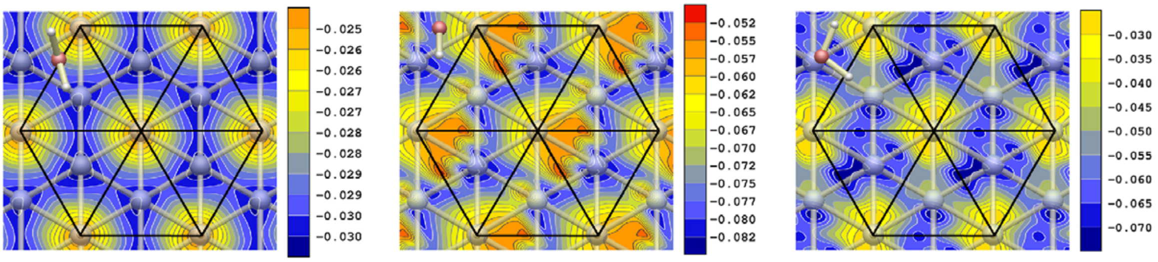

Fig. 1. Potential energy surfaces (adsorption energy in eV with respect to gas-phase water) in dependence of the initial orientations of the water molecule. In the left/middle panel the O/one H atom point towards the surface. Right the case of a molecular plane parallel to the surface is shown. The H_2O oxygen serves as molecular point of reference.